PREDICTING THE POTENTIAL SUITABLE HABITAT FOR *TAMARIX CHINENSIS* UNDER CLIMATE CHANGE BASED ON CMIP6 IN CHINA

WU, C. W.[1] – XU, X. X.[1,2*] – ZHANG, G. J.[1,2] – CHENG, B. B.[1,2] – HAN, S.[1]

[1]*College of Horticulture Science and Technology, Hebei Normal University of Science & Technology, Qinhuangdao 066600, PR China*

[2]*Hebei Key Laboratory of Horticultural Germplasm Excavation and Innovative Utilization, Qinhuangdao 066600, PR China*

[*]*Corresponding author*
e-mail: xuxingxing0317@126.com

(Received 21st Jan 2022; accepted 2nd May 2022)

Abstract. *Tamarix chinensis* (Tamaricaceae), a halophytic plant, is native to China. *Tamarix chinensis* has shown significant advantages in improving soil desertification and enhancing soil quality in coastal saline lands and can be used for ornamental and medicinal purposes with high scientific, ecological and economic values. The scarcity of information about geographic distribution under global climate change makes it difficult to promote better cultivation of this shrub. For this study, we modeled the current and future suitable growth areas in 2050 and 2070 for *T. chinensis* by the Maxent model using the latest Coupled Model Comparison Program 6 (CMIP6) data set. The results revealed that annual mean temperature, precipitation of wettest quarter, annual mean UV-B and elevation were identified as the most important factors affecting *T. chinensis* distribution. The total suitable potential distribution areas for *T. chinensis* encompassed ca. 191.38×10^4 km^2, in which the highly suitable areas were mainly distributed in the middle and lower reaches of the Yellow River and the eastern coastal areas in China. Under the Shared Socioeconomic Pathway (SSP) 126 scenario, we predicted an expansion of the suitable habitat range in 2050 followed by a contraction in 2070; however, under the SSP585 scenario, the suitable habitat range of *T. chinensis* would decrease in 2050 and 2070. Overall, *T. chinensis* showed a shift trend in distribution to higher latitudes and elevations with global warming. This study could provide a theoretical guidance for formulating management plans for *T. chinensis* and saline soil rehabilitation in the future.
Keywords: *halophyte, environmental factor, species distribution, habitat shift, SSPS*

Introduction

Global climate change has already affected ecosystems and biological species (Kozak et al., 2008). According to the report of the Intergovernmental Panel on Climate Change (IPCC), the average global surface temperature has risen by 0.85°C during 1980–2012 (IPCC, 2013). Thus, global warming has become an indisputable fact. A continuous and more rapid warming trend has been simulated by multiple climate models, which predicted that the global surface temperature will increase by 1–6°C by the end of the 21st century, relative to pre-industrial temperature levels (Rogelj et al., 2012). A number of studies have shown that climate change has altered the current habitat suitability and spatial distribution patterns of many species, and even led to the migration and extinction of some organisms (Bertrand et al., 2011; Anderegg et al., 2015; Feng et al., 2021). Therefore, it is very important for predicting the potential distribution of species under global climate change. Understanding the spatial patterns

http://www.aloki.hu ● ISSN 1589 1623 (Print) ● ISSN1785 0037 (Online)
DOI: http://dx.doi.org/10.15666/aeer/2004_28452863

of species and their dependence on the climate factors is very useful for planning strategies to use resources sustainably in the future (Liu et al., 2018).

To better analyze the frequency and intensity of climate change, the sixth phase of the Coupled Model Comparison Program (CMIP6) has been formulated scientifically based on the scientific gaps learned from CMIP5 in 2021 (Bai et al., 2021). The current CMIP6 models differ from those of CMIP5 due to a new generation of climate models in which a new set of emission scenarios are driven by shared Socioeconomic Pathways (SSPs) for further analysis (Gidden et al., 2019; Liang et al., 2020). CMIP6 models are expected to be more reliable (Eyring et al., 2016; Zhang et al., 2021) because higher transient climate response and climate sensitivity compared to earlier models in CMIP5, with stronger warming in recent decades (Zelinka et al., 2020; Liang et al., 2020). In addition, CMIP6 showed higher accuracy statistics, particularly in annual and seasonal mean temperature and precipitation compared to CMIP5 (Bağçaci et al., 2021). It is of great benefit to researchers and decision makers to provide a guide for the distribution of plantations under the new emission scenarios in the future.

Species distribution models (SDMs) are used as effective tools in analyzing the impact of climate change on the potential distribution of species (Elith et al., 2006; Peterson, 2007). At present, the maximum entropy model (Maxent) has become one of the most frequently used niche models compared to other models, such as biological population growth model (CLIMEX), Domain and genetic algorithm for rule set production (GARP) (Zhang et al., 2018). It builds a prediction model based upon current species distribution records and environmental variables (Elith et al., 2011). Due to its small sample size and superior performance, the Maxent model has become an ideal prediction tool that can meet different research objectives (Phillips and Dudík, 2008; Pearson et al., 2011). For example, numerous studies based on Maxent modeling were conducted on endangered species conservation (Chen et al., 2020; Wei et al., 2020; Lu et al., 2021), invasive species control (Zhang et al., 2021) and planting suitability regionalization (Peng et al., 2019; Xu et al., 2020).

Climate change is considered one of the major contributing factors to soil salinization that leads to environmental degradation (Rogel et al., 2000). Approximately 6.5% of the world's total land area is affected by salinization until 2020 (Munns and Tester, 2008; Litalien and Zeeb, 2020). Soil salinity can strongly affect seed germination and plant growth and directly threat the function of many ecosystems (Santos et al., 2016). Halophytes could not only survive and reproduce in environments where the salt concentration is 200 mM NaCl or more (Flowers and Colmer, 2008) but survive under other harsh conditions, including drought, cold or flooding (Fan, 2020). Therefore, halophytes play an important role in ecological restoration of salt-affected land and minimizing soil degradation (Litalien and Zeeb, 2020).

Tamarix chinensis Lour., is one of the native halophytes usually distributed in China's warm-temperate zone. It is a perennial shrub or small tree with scalelike leaves and racemes of pink flowers (*Figure 1a, 1b*). In order to adapt to complex hypersaline environments, *T. chinensis* has evolved special salt-secreting structures - salt glands, *T. chinensis* can secrete excess salt out of its body via salt glands to avoid excessive salt absorption (*Figure 1c*) (Jiang et al., 2012). With properties of strong salt and drought resistance, *T. chinensis* plays a pivotal role in maintaining ecosystem stability in saline lands (Sun et al., 2020). Thus, it is of unique scientific research value and ecological significance. Additionally, *T. chinensis* has high ornamental value and can be used for landscaping applications. Currently, *T. chinensis* is undergoing population declination

http://www.aloki.hu ● ISSN 1589 1623 (Print) ● ISSN1785 0037 (Online)
DOI: http://dx.doi.org/10.15666/aeer/2004_28452863

and fragmentation due to climate change and human disturbance (Sun et al., 2020). Therefore, it acts as an ideal model species for studying the impact of climate change on species distribution. Predictions of potential distribution of species under global climate change play an instructional role for introduction and sustainable resource use (Peterson et al., 2011; Du et al., 2020). Therefore, *T. chinensis* as a representative species of strong salt and drought resistance plants, Research on *T. chinensis* is urgent and necessary. Predicting the potential distribution of *T. chinensis* under global climate change can provide an important reference for the future introduction and application of *T. chinensis*, maximising the ecological value of the species. However, to my knowledge, there is very limited studies using CMIP6 data set to predict the potential geographic distribution under future climate change scenarios.

Figure 1. *Appearance. (a) racemes of pink flowers (b) scale-like leaves (c) Salt glands*

In this study, Maxent modeling were used to predict distribution of *T. chinensis* in China based on an extensive collection of geo-referenced occurrence records of *T. chinensis* and associated environmental data for current and future climate scenarios using the current CMIP6 data. The aims of this research were to: (1) identify the main environmental variables affecting the potential distribution of *T. chinensis*; (2) to predict the potential distribution of *T. chinensis* in current and future (2050s and 2070s) climate conditions under the lowest and the highest limits of the Shared Socio-economic Pathways (SSP126 and SSP585); (3) to determine the habitat shift of the core distribution area of *T. chinensis* under 2050s and 2070s climate scenarios. The results will provide a reference for introducing and cultivating *T. chinensis* resources across China.

Material and methods

Species occurrence data for T. chinensis

In this paper, the native records were obtained from three resources: (1) field survey during 2018 in China, (2) the specimen libraries including the Global Biodiversity Information Facility (https://www.gbif.org/), the National Specimen Information

http://www.aloki.hu ● ISSN 1589 1623 (Print) ● ISSN1785 0037 (Online)
DOI: http://dx.doi.org/10.15666/aeer/2004_28452863

Infrastructure (http://www.nsii.org.cn) and the Chinese Virtual Herbarium (http://www.cvh.ac.cn/), (3) the reports in literatures (Zhang et al., 2019; Sun et al., 2020).

Environmental variables

Initially, 30 environmental variables were chosen to model the current species distribution (*Table S1*). These included 19 bioclimatic variables for the period from 1970 to 2000 obtained from the World Climate Database (WorldClim 2.1 released in January 2020, http://www.worldclim.org/) (Fick and Hijmans, 2017). In addition, topographical data were downloaded from the Geospatial Data Cloud (http://www.gscloud.cn/) to generate the elevation(Alt), slope (Slop) and aspect (Asp) data layers; soil data (T_OC, T_PH_H_2O, T_TEB and T_USDA_TEX_CLASS) were from the soil characteristics database (http://globalchange.bnu.edu.cn/research/soil2) (Shang et al., 2013) and Global ultraviolet-B radiation (UVB 1–4) were from the gIUV database (http://www.ufz.de/gliv/) (Beckmann et al., 2014). These environmental variables were extracted from the base map of China that was obtained from the National Fundamental Geographic Information System website (http://nfgis.nsdi.gov.cn/) by ArcGIS 10.5 at 2.5 minutes (approximately 5 km^2) spatial resolution.

For future climate scenarios, we used BCC-CSM2-MR climate change modeling data (a middle resolution climate system model developed by Beijing) from the new CMIP6 database (Eyring et al., 2016; Jamal et al., 2020). The SSP126 and the SSP585 at 2.5 minutes spatial resolution were used for two future periods: 2041-2060 (2050) and 2061-2080 (2070) (http://www.worldclim.org/). The SSP126 represents the low-emission scenario measured by its radiative forcing pathway and predicted a warming inferior to 2°C by 2100. The SSP585 is a high-emission scenario that stabilized radiative forcing at 8.5 W/m2 in 2100 (Riahi et al., 2017). The Eleven parameters (three topographical variables, four soil and four UV-B radiation parameters) remained unchanged to predict the influence of future climate changes on the distribution of *T. chinensis*.

To reduce multicollinearity of these variables and overfitting of the Maxent model (Graham, 2003), highly correlated environmental factors ($r \geq 0.80$ Pearson' correlation coefficients) were removed from the prediction models (*Table S2*). Finally, 14 environmental variables were selected by ArcGIS 10.5 (Eris, Redlands California, USA) for the Maxent model. These 14 variables included annual mean temperature (Bio1), temperature annual range (Bio7), precipitation of the driest month (Bio14), precipitation seasonality (Bio15) and precipitation of wettest quarter (Bio16), elevation (Alt), slope (Slop), aspect (Asp), topsoil organic carbon (T_OC), topsoil pH (T_PH_H_2O), topsoil TEB (T_TEB), topsoil USDA texture classification (T_USDA_TEX_CLASS), annual mean UV-B (UVB1) and UV-B seasonality (UVB2) (*Table 1*).

Maxent model processing

The current and future distribution of *T. chinensis* in China was analyzed using the maximum entropy modeling in Maxent v 3.4.1 (Phillips et al., 2020). We ran 20 replicates with randomly 25% of the location points used for model testing and determined logistic probabilities for the output. Other parameter settings were kept as default.

http://www.aloki.hu ● ISSN 1589 1623 (Print) ● ISSN1785 0037 (Online)
DOI: http://dx.doi.org/10.15666/aeer/2004_28452863

Table 1. *The contribution proportions and permutation importance of the 14 environmental variables included in the Maxent models for T. chinensis*

Code	Environmental variables	Contribution (%)	Permutation importance
Bio1	Annual mean temperature	39.0	42.7
Bio16	Precipitation of wettest quarter	18.8	19.3
UVB1	Annual mean UV-B	10.2	10.8
Alt	Elevation	7.5	15.8
UVB2	UV-B seasonality	7.3	1.2
T_PH_H2O	Topsoil pH (H2O)	5.8	0.3
Bio7	Temperature annual range (BIO5-BIO6)	5.2	1.6
Slop	Slope	2.4	2.1
Bio15	Precipitation seasonality (coefficient of variation)	1.9	1.3
Bio14	Precipitation of driest month	0.6	2.0
T_USDA	Topsoil USDA texture classification	0.5	1.5
Asp	Aspect	0.4	0.6
T_TEB	Topsoil TEB	0.3	0.7
T_OC	Topsoil organic carbon	0.1	0.1

To evaluate the model's predictive performance, the area under receiver operating characteristic curve (AUC) values were examined. Generally, AUC values between 0.7 and 0.9 were considered to have a very good fit, and higher than 0.9 were considered as a perfectly fitted model (Wei et al., 2020; Xu et al., 2020). The Jackknife test was used to analyze the contribution rate and importance of these environmental variables. Moreover, the most important variables used in the model were analyzed in regard to their response curves.

Determining the environmentally suitable cultivation areas

For further analysis, the outputs of the Maxent models were transformed into raster format predicting the presence of *T. chinensis* (0–1 range) using ArcGIS 10.5. A presence–absence map was produced using the "Maximum training sensitivity plus specificity". threshold which has been shown to produce highly accurate predictions (Peng et al., 2019; Xu et al., 2019). Finally, we divided the habitat suitability maps into four classes with the "Maximum training sensitivity plus specificity" value of 0.30: unsuitable habitat (0–0.30); poorly suitable habitat (0.30–0.50); moderately suitable habitat (0.50–0.70) and highly suitable habitat (0.70–1.0). For each model, we calculated the suitable habitat area by the proportion of the data set.

The core distributional shifts

The "QuickReclassify to Binary" in the SDMtoolbox v2.4 tool kit (Brown and Barbara, 2014) was used to convert the raster file into a binary file, and then we converted the binary file to the ". asc" file. The "Centroid Changes (Lines)" tool was used to calculate the displacement of the geometric center of current and future suitable areas. Finally, the overall change trend of the distribution area of *T. chinensis* were tracked.

http://www.aloki.hu ● ISSN 1589 1623 (Print) ● ISSN1785 0037 (Online)
DOI: http://dx.doi.org/10.15666/aeer/2004_28452863

Results

Model performance and major environmental variables

For the current distribution, the average omission rate is close to the predicted omission for the training presence records and the test records (*Figure S1*). In addition, the mean AUC value for the Maxent models was 0.857, it was higher than the AUC value of a random prediction (*Figure S2*). This indicated the model had good predictive accuracy and good performance for modelling the geographic distribution of *T. chinensis* in China.

The importance of the relative contributions of environmental variables to the Maxent model was evaluated using the jackknife test in *Figure 2*. Among the 14 variables, the most important factors affecting the habitat distribution of *T. chinensis* were annual mean temperature (Bio1, 39.0%), precipitation of wettest quarter (Bio16, 18.8%), annual mean UV-B (UVB1, 10.2%), elevation (Alt, 7.5%) and UV-B seasonality (UVB2, 7.3%). The cumulative contributions of these five parameters reached values as high as 82.8% (*Table 1*).

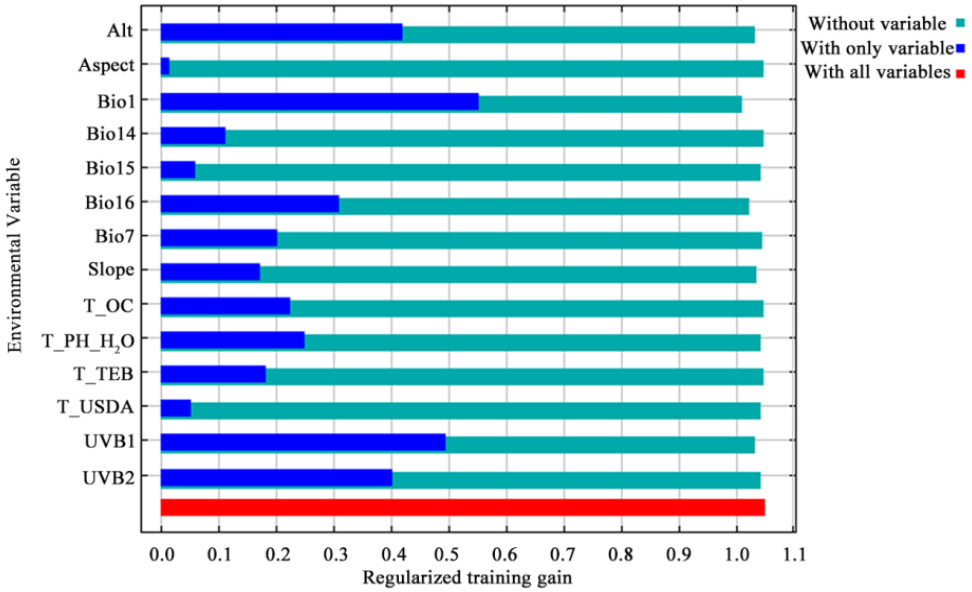

Figure 2. *Jackknife test evaluating the relative importance of environmental variables on the distribution of T. chinensis*

Based on the response curves (*Figure 3*), the thresholds (existence probability>0.3) of the major ecological factors were obtained: annual mean temperature (Bio1) ranged from 5.6 to 16.7°C, precipitation of wettest quarter (Bio16) ranged from 116 to 860 mm and from 860-1086 mm, UVB1 ranged from 2284 to 3238 $J.m^{-2}.day^{-1}$, UVB2 ranged from 1.27 to 1.75 $J \cdot m^{-2} \cdot day^{-1}$, and elevation (Alt) was from -124m to 2659 m.

Predicted current potential distribution of T. chinensis

In China, *T. chinensis* is naturally distributed in warm-temperate zone, including Hebei, Shandong, Liaoning, Jiangsu provinces (Sun et al., 2020), inhabiting river beds, sandy floodplains, deserts, and coastal tidal flats (Zhang et al., 2019). A total of 381

http://www.aloki.hu ● ISSN 1589 1623 (Print) ● ISSN1785 0037 (Online)
DOI: http://dx.doi.org/10.15666/aeer/2004_28452863

known occurrences of *T. chinensis* were obtained for constructing the models (*Figure 4a*). The current potential distribution of *T. chinensis* in China was illustrated in *Figure 4b*. The results showed that the total suitable area was about 191.38×10^4 km^2, accounting for 19.94% of the total area of China, and the poor, moderate and high suitable areas accounted for 53.87%, 39.06%, and 7.07% of the total suitable area, respectively (*Table 2*). The areas with habitats suitability above 30% were mainly distributed in the middle and lower reaches of the Yellow River and the eastern coastal regions. Currently the highly suitable areas were distributed in the Hebei Province, the northeast of Shandong Province, the north of Henan Province, the coastal areas of Tianjin city and Liaoning Province.

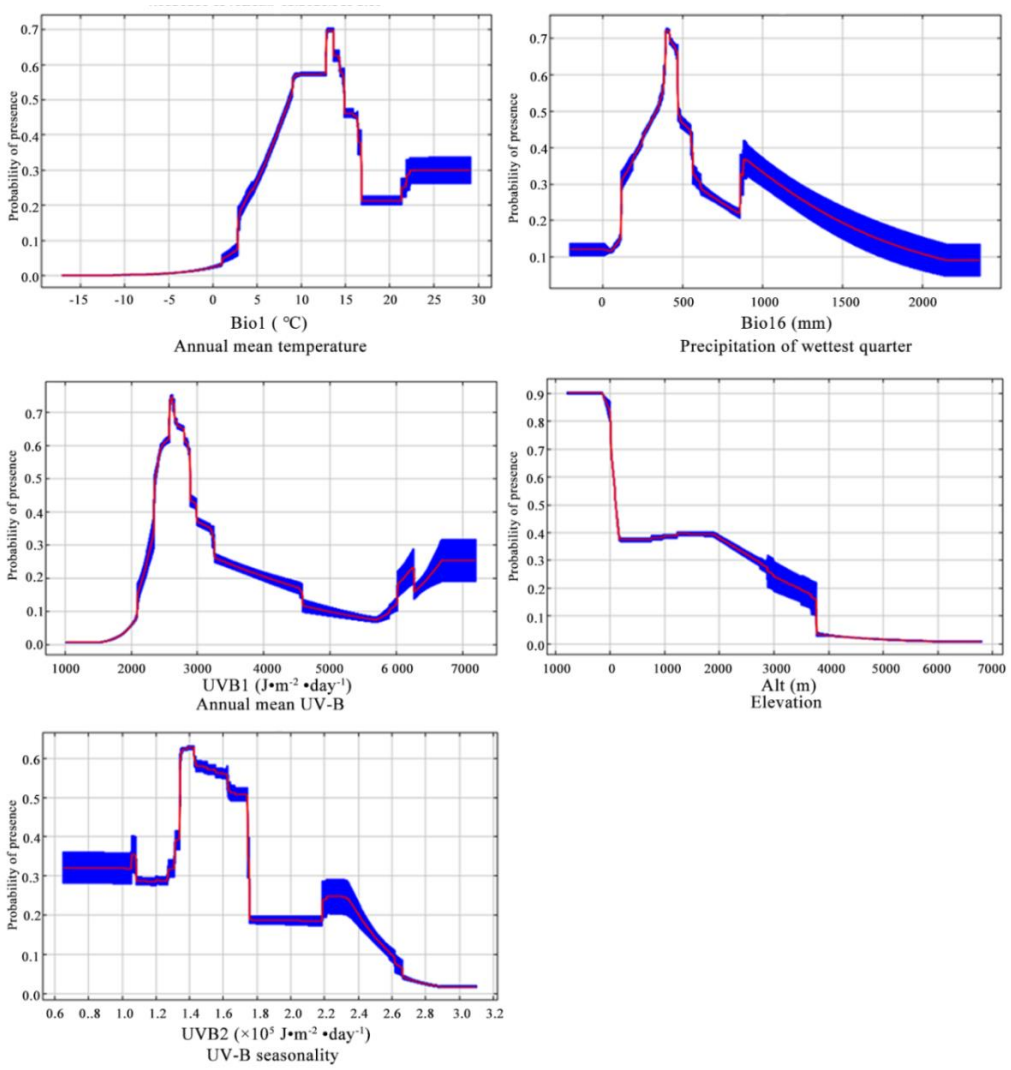

Figure 3. *Response curves for important environmental variables affecting the distribution of T. chinensis in China. Annual mean temperature (Bio1), precipitation of wettest quarter (Bio16), annual mean UV-B (UVB1), UV-B seasonality (UVB2), and elevation (Alt). The red curves are the averages and blue margins show one standard deviation (SD) calculated over the 20 replicates*

http://www.aloki.hu ● ISSN 1589 1623 (Print) ● ISSN1785 0037 (Online)
DOI: http://dx.doi.org/10.15666/aeer/2004_28452863

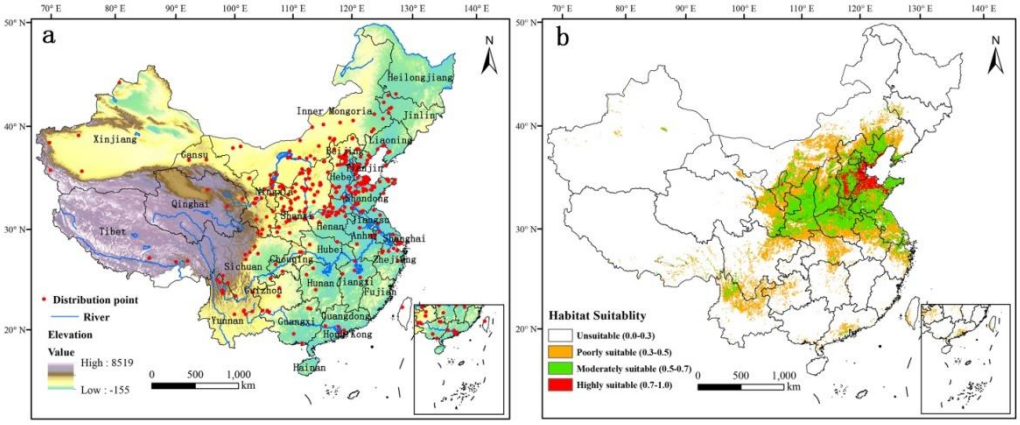

Figure 4. *(a) Geographic locations of Tamarix chinensis occurrences in China. Red point shows the species occurrence location. (b) The potential distribution of T. chinensis under current climate conditions in China using the Maxent model. The red colour indicates areas with a high probability of occurrence for T. chinensis, the green colour represents a moderate probability of occurrence, the orange colour represents a low probability of occurrence, and the white colour indicates areas not suitable for T. chinensis*

Table 2. *Suitable areas for T. chinensis under different climate change scenarios (10^4 km^2)*

Period	Poorly suitable	Moderately suitable	Highly suitable	Total suitable
Current	103.10	74.75	13.54	191.38
2050s, SSP126	105.82	73.90	12.96	192.68
2070s, SSP126	98.90	73.76	14.08	186.74
2050s, SSP585	97.59	75.23	13.05	185.87
2070s, SSP585	97.74	70.98	14.86	183.58

Potentially suitable climatic distributions in the future

We used the Maxent models to predict the suitable distribution areas of *T. chinensis* in China in the future (2050 and 2070) under the lowest and the highest future SSP scenarios (SSP126 and SSP585) (*Figure 5*). Under the SSP126 climate scenario, the total area of *T. chinensis* increased slightly in the 2050s, amounting to ca. 192.68×10^4 km^2 (*Table 2*). Maxent estimated that the increased distribution area is 17.89×10^4 km^2, the decreased area is 16.36×10^4 km^2, and the stable area is 169.48×10^4 km^2 (*Table 3*). The newly suitable habitats mainly appear in the southern sector of Inner Mongolia, the northern Shanxi, Liaoning, as well as in the Yangtze River Basin. Losses in suitable areas appear mainly in northern of Mongolia, Gansu, Yunnan, Hubei, Anhui and Zhejiang Provinces (*Figure 5*). However, the total area decreased in the 2070s (186.74×10^4 km^2). Interestingly, in 2070, the highly suitable area was 3.99% higher than the current highly suitable area (*Table 2*). And the increased area is 10.85×10^4 km^2, the loss area is 15.71×10^4 km^2, and the stable area is 170.48×10^4 km^2 (*Table 3*).

Under the SSP585 climate scenario, the total area of *T. chinensis* decreased both in the 2050s (185.87×10^4 km^2) and in the 2070s (183.58×10^4 km^2) (*Table 2*). Overall, the increased and decreased habitat stayed generally stable as under SSP126 (*Figure 5*). In

http://www.aloki.hu ● ISSN 1589 1623 (Print) ● ISSN1785 0037 (Online)
DOI: http://dx.doi.org/10.15666/aeer/2004_28452863

2050s, the area of increased, decreased and unchanged habitat is 11.88×10^4 km^2, 17.56×10^4 km^2 and 168.28×10^4 km^2, respectively. In 2070, the increased area and the decreased area increase to 14.11×10^4 km^2 and 22.05×10^4 km^2, respectively (*Table 3*).

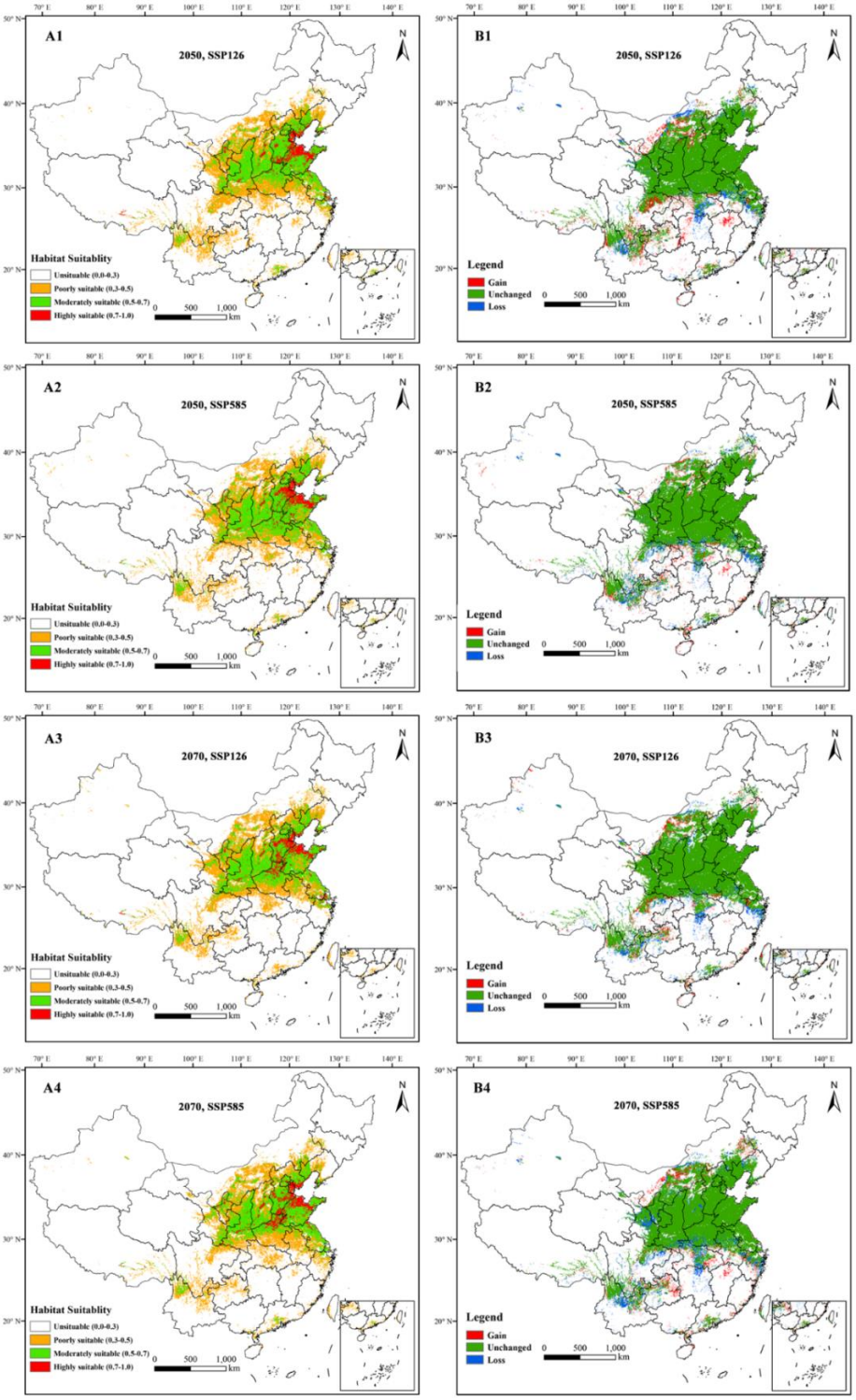

Figure 5. *Future species distribution models of T. chinensis under climate change scenarios SSP126 and SSP585 in China. A1-A4, future suitable habitats distribution of T. chinensis; B1-B4, Comparison between the current and the future climate scenarios*

http://www.aloki.hu ● ISSN 1589 1623 (Print) ● ISSN1785 0037 (Online)
DOI: http://dx.doi.org/10.15666/aeer/2004_28452863

Table 3. *Dynamic changes in suitable habitat area for T. chinensis under four future climate scenarios (10^4 km^2)*

Period	Decreased	Increased	Unchanged
2050s, SSP126	16.36	17.89	169.48
2070s, SSP126	15.71	10.85	170.14
2050s, SSP585	17.56	11.88	168.28
2070s, SSP585	22.05	14.11	163.79

Core distribution shifts

To grasp an overall understanding of distribution shifts, the centroids of both the current and future were calculated and drawn (*Figure 6*). The centroid of the current habitat of *T. chinensis* was predicted to be located in south Shanxi province (112.267 E and 35.61 N). Under SSP 126, it might shift southwest in 2050 (111.953 E and 35.611 N), but north in 2070 (112.129 E and 35.638 N). Overall, the core distribution of the two climate scenarios under SSP 126 showed a westward-shifting trend. Meanwhile, under SSP 8.5 the centroid of the suitable area was predicted to shift northwest in 2050 (112.192 E and 35.671 N) and then might move east in 2070 (112.524 E and 35.67 N). Overall, the core distribution of the two climate scenarios under SSP 585 showed a northward-shifting trend.

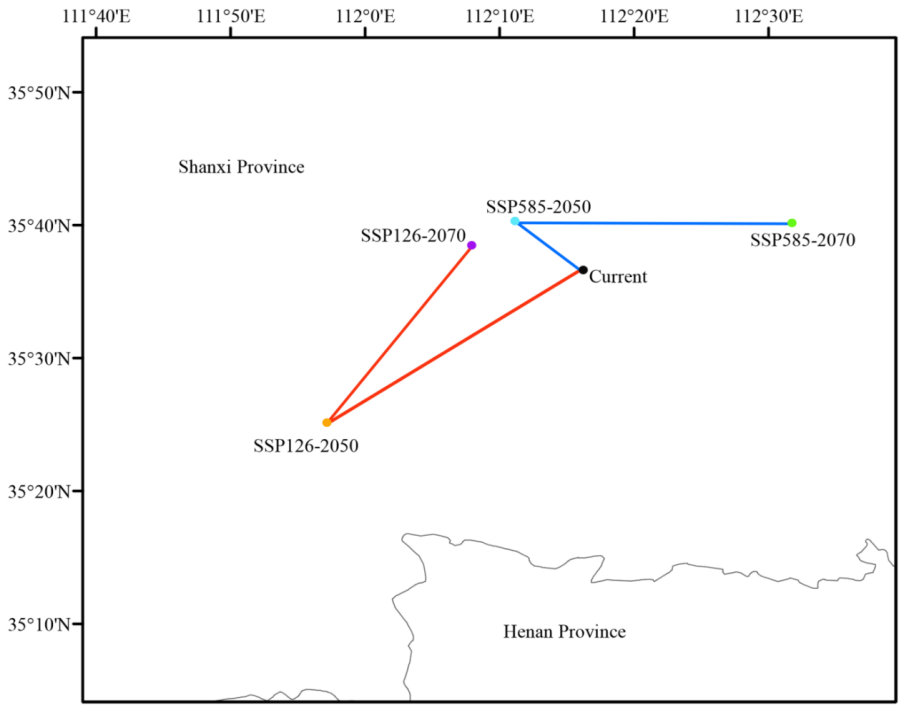

Figure 6. *Potential habitats shifts of T. chinensis under different climate change scenarios. Black dot indicates the geometric center of suitable area under current climate condition; orange dot and purple dot indicate the geometric centers of future suitable areas of 2050 and 2070 under the climate scenario of SSP126; blue dot and green dots indicate the geometric centers of future suitable areas of 2050 and 2070 under the climate scenario of SSP585*

http://www.aloki.hu ● ISSN 1589 1623 (Print) ● ISSN1785 0037 (Online)
DOI: http://dx.doi.org/10.15666/aeer/2004_28452863

Discussion

Climate change could impact geographical distribution of species (Zhang et al., 2018). *T. chinensis* is one of the most highly salt-tolerant shrub species with 340 Mm NaCl limit (Ye et al., 2020). As a native halophyte, it shows the wide adaptability to different ecological environment such as flooded, salty and arid conditions in China (Zhang et al., 2019). For this study, Maxent and ArcMap software have been used to predict the potential geographic distribution of *T. chinensis* under current and future climate scenarios based on the latest CMIP6 data set which is very important for assessing the suitable cultivation areas and formulating management plans.

The AUC values tested by the Maxent model were more than 0.7, which showed a good fit of the used model (Philips et al., 2006; Wei et al., 2020; Xu et al., 2020). In this study, the mean AUC value for the Maxent models was 0.857, indicating that the model had good predictive accuracy. Moreover, the prediction result and the actual distribution of *T. chinensis* remained consistent in China.

Under the current climate, *T. chinensis* had a wide but sporadic distribution in China. This model was consistent with the previous occurrence records that located in Liaoning, Jiangsu, Shandong, Hebei, Anhui, Henan, and some regions of Shanxi and Gansu etc. (Sun et al., 2020). There are only small differences between the applied scenarios in terms of the predicted area suitable for *T. chinensis* but this could be the reason for the high adaptability of the species. Our results showed that the total potential distribution area of *T. chinensis* was about 191.38×10^4 km^2 under current climate, in which the highly suitable areas were mainly distributed in the middle and lower reaches of the Yellow River and the eastern coastal regions.

In the current model, according to the contribution proportions of environmental factors and the jackknife test, annual mean temperature, precipitation of wettest quarter, annual mean UV-B and elevation were the most important factors affecting the distribution of *T. chinensis*. Studies have showed that the distribution of *T. chinensis* was largely affected by mean temperature of coldest quarter and precipitation of warmest quarter (Sun et al., 2020). Populations with rich genetic diversity usually existed at lower altitudes, in warmer habitats, and in eastern regions nearer to the sea (Sun et al., 2019). The model species has a wide adaptation capacity. It is confirmed by the wide range of the analysed environmental variables. The maximum acceptable mean temperature is approximately three times higher than the minimum and the differences in the precipitation of the wettest quarter is approximately fourfold.

Temperature affects the seed germination of *T. chinensis*, and it showed that an extremely cold (<5°C) and high temperature (>45°C) were found to be unfavorable for seed germination (Wang et al., 2006). The precipitation of wettest quarter (Bio16) is from 116 to 1086mm, which showed that an extremely dry climate was not suitable for this species. This was consistent with the result of a study that the occurrence of *Tamarix* spp. was positively correlated to precipitation of the warmest quarter (Cord et al., 2010). Previous study has also shown that the soil moisture was the main environmental factor that affected the distribution of *Tamarix gansuensis* (Zhao et al., 2018). Water is a basic requirement for seed. Seeds of *T. chinensis* are light and small, with hairs on the epidermis, making them highly suited to dispersal to different distances by water. In summer, the seeds of *T. chinensis* usually germinate within 24 h in moist soil, even when afloat seedlings could survive submerged for a few weeks (Jiang et al., 2012; Jiao et al., 2021). In addition, the groundwater affects the leaf

http://www.aloki.hu ● ISSN 1589 1623 (Print) ● ISSN1785 0037 (Online)
DOI: http://dx.doi.org/10.15666/aeer/2004_28452863

photosynthetic efficiency of *T. chinensis* by significantly impacting the soil water content within the distribution range of the root system (Xia et al., 2020).

In this study, the elevation and UV-B radiation were also the important factors affecting the distribution of *T. chinensis*. According to the response curves (existence probability > 0.70), the highly suitable elevation value was from 0 to 171 m. This is in accordance with previous results (Song et al., 2010; Sun et al., 2016), in which populations existed in eastern regions nearer to the sea, where are characterized by low elevation. UV-B radiation has a significant influence on the growth and performance of terrestrial plants (Garcia-Corral et al., 2017; Díaz- Guerra et al., 2019). It may can lead to changes at the cellular and organismal scales, inducing a variety of morphological, physiological, and molecular responses in plants (Valle et al., 2020). However, little is known about how *T. chinensis* respond to UV-B radiation.

With global warming, most species may generally migrate to higher latitudes and elevations (Zhang et al., 2018; Peng et al., 2019). A study in the northeastern United States revealed that the distribution of forests was shifting northward with climate change (Wang et al., 2017). High-alpine species are expanding their range to higher altitudes in respond to climate change (Rumpf et al., 2018). Consistently, the core distribution of *T. chinensis* showed a westward-shifting trend under SSP126 and a northward-shifting trend under SSP585. New suitable habitats would appear in the southern sector of Inner Mongolia, the northern Shanxi and Liaoning. Overall, the centroids of suitable habitat shifted was higher than the current area, which indicated that *T. chinensis* will be able to adapt to climate change.

Under the SSP126 scenario, we predicted suitable habitat range of *T. chinensis* increased in 2050 followed by decreased in 2070. The predicted increase and decrease in the suitable habitat is almost the same, this indicates that the restructuration of the habitats is predicted but large changes in the overall distribution are not expected. Under the SSP 585 scenario, suitable habitat range was predicted to decrease with the increased intensity of global warming, which suggested *T. chinensis* could not benefit from global warming. A continuous rise in temperature might had a negative effect on plants (Xu and Xue, 2013; Zhang, 2018). Losses in suitable areas may be at great risk of soil salinization and aridification under global warming (Sun et al., 2020). The habitat suitability of *T. chinensis* was affected not only by environmental factors, but also by intraspecific facilitation, wind dispersal of seeds and human activities. The intensive dispersal and germination in the short term resulted in habitat fragmentation (Jiao et al., 2021). Additionally, unsustainable land use and management could lead to a decrease in suitable habitat of *T. chinensis*.

Generally, assessment of habitat suitability plays an instructional role for the identification of future suitable areas and cultivation of *T. chinensis*. In this study, the moderate and high suitable areas should be given priority for cultivation of *T. chinensis*. In addition, new habitats in higher latitudes and elevations in the future such as Liaoning province, the southern sector of Inner Mongolia province and north of Shanxi should also be considered as suitable habitats for *T. chinensis* introducing.

Conclusions

To assess the impact of climate change on the distribution of *T. chinensis*, we modeled the current and future potential distribution using the Maxent model based on the latest CMIP6 data. Annual mean temperature, precipitation of wettest quarter,

http://www.aloki.hu ● ISSN 1589 1623 (Print) ● ISSN1785 0037 (Online)
DOI: http://dx.doi.org/10.15666/aeer/2004_28452863

annual mean UV-B and elevation were the most important factors affecting the distribution of *T. chinensis*. Under the SSP126 scenario, we predicted suitable habitat range of *T. chinensis* increased in 2050 followed by decreased in 2070; however, under the SSP585 scenario, we predicted that the suitable habitat range would decrease with the increased intensity of global warming. Overall, the core distribution of *T. chinensis* showed a westward-shifting trend under SSP 126 and a northward-shifting trend under SSP 585. The predicted spatial and temporal shift patterns of *T. chinensis* will provide a useful reference for assessing the suitable cultivation areas and sustainable resource use of *T. chinensis*.

Declaration of competing interests. The authors declare that they have no known competing financial interests or personal relationships that could have appeared to influence the work reported in this paper.

Acknowledgments. This work was funded by the Doctoral Scientific Research Foundation of Hebei Normal University of Science & Technology (2019YB016), Hebei Provincial Department of Science and Technology Project (21326346D), National Finance Forestry Science and Technology Promotion and Demonstration Project (TG [2020]005), Science and Technology Research Project for Higher Schools in Hebei Province (ZD2022091), Graduate Innovation Project of Educational Committee of Hebei Province of China (CXZZSS2022095).

REFERENCES

[1] Anderegg, W. R. L., Hicke, J. A., Fisher, R. A., Allen, C. D., Aukema, J., Bentz, B., Hood, S., Lichstein, J. W., Macalady, A. K., McDowell, N., Pan, Y., Raffa, K., Sala, A., Shaw, J. D., Stephenson, N. L., Tague, C., Zeppel, M. (2015): Tree mortality from drought, insects, and their interactions in a changing climate. – New. Phytol 208: 674-683.

[2] Bağçaci, S. Ç., Yucel, I., Duzenli, E., Yilmaz, M. T. (2021): Intercomparison of the expected change in the temperature and the precipitation retrieved from CMIP6 and CMIP5 climate projections: A Mediterranean hot spot case, Turkey. – Atmospheric Research 256: 105576.

[3] Bai, H., Xiao, D., Wang, B., Liu, D. L., Feng, P., Tang, J. (2020): Multi-model ensemble of CMIP6 projections for future extreme climate stress on wheat in the North China plain. – RMetS, International Journal of Climatology 41(S1): E171-E186. DOI: https://doi.org/10.1002/joc.6674.

[4] Beckmann, M., Vaclavik, T., Manceur, A. M., Sprtova, L., von Wehrden, H., Welk, E., Cord, A. F. (2014): glUV: A global UV-B radiation data set for macroecological studies. – Methods Ecol Evol 5: 372-383.

[5] Bertrand, R., Lenoir, J., Piedallu, C., Riofrío-Dillon, G., Ruffray, P. D., Vidal, C., Pierrat, J. C., Gégout, J. C. (2011): Changes in plant community composition lag behind climate warming in lowland forests. – Nature 479: 517-520.

[6] Brown, J. L., Barbara, A. (2014): SDMtoolbox: a python-based GIS toolkit for landscape genetic, biogeographic and species distribution model analyses. – Methods Ecol Evol 5: 694-700.

[7] Chen, Q. H., Yin, Y. J., Zhao, R., Yang, Y., Silva, J., Yu, X. N. (2020): Incorporating local adaptation into species distribution modeling of Paeonia mairei, an endemic plant to China. – Front Plant Sci 10.

[8] Cord, A., Klein, D., Dech, S. (2010): Remote Sensing Time Series for Modeling Invasive Species Distribution: A Case Study of Tamarix spp. in the US and Mexico. – International Congress on Environmental Modelling and Software 556.

[9] Díaz-Guerra, L., Llorens, L., Bell, T. L., Font, J., González, J. A., Verdaguer, D. (2019): Physiological, growth and root biochemical responses of Arbutus unedo and Quercus

http://www.aloki.hu ● ISSN 1589 1623 (Print) ● ISSN1785 0037 (Online)
DOI: http://dx.doi.org/10.15666/aeer/2004_28452863

suber seedlings to UV radiation and water availability before and after aboveground biomass removal. – Environ Exp Bot 168: 103861.

[10] Du, Z. Y., He, Y. M., Wang, H. T., Wang, C., Duan, Y. Z. (2020): Potential geographical distribution and habitat shift of the genus Ammopiptanthus in China under current and future climate change based on the Maxent model. – J Arid Environ 184: 104328.

[11] Elith, J., Graham, C. H., Anderson, R. P., Dudik, M., Ferrier, S., Guisan, A., Hijmans, R. J., Huettmann, F., Leathwick, J. R., Lehmann, A., Li, J., Lohmann, L. G., Loiselle, B. A., Manion, G., Moritz, C., Nakamura, M., Nakazawa, Y., Overton, J. M. M., Peterson, A. T., Phillips, S. J., Richardson, K., Scachetti-Pereira, R., Schapire, R. E., Soberón, J., Williams, S., Wisz, M. S., Zimmermann, N. E. (2006): Novel methods improve prediction of species' distribution from occurrence data. – Ecography 19: 129-151.

[12] Elith, J., Phillips, S. J., Hastie, T., Dudik, M., Chee, Y. E., Yates, C. J. (2011): A statistical explanation of MaxEnt for ecologists. – Divers. Distrib. 17: 43-57.

[13] Eyring, V., Bony, S., Meehl, G. A., Senior, C. A., Stevens, B., Stouffer, R. J., Taylor, K. E. (2016): Overview of the Coupled Model Intercomparison Project Phase 6 (CMIP6) experimental design and organization. – Geosci Model Dev 9: 1937-1958.

[14] Fan, D. L., Zhong, H. L., Hu, B., Tian, Z., Sun, L. X., Fischer, G., Wang, X. Y., Jiang, Z. Y. (2020): Agro-ecological suitability assessment of Chinese Medicinal Yam under future climate change. – Environ. Geochem Health 42(3): 987-1000.

[15] Feng, L., Sun, J. J., Wang, T. L., Tian, X. N., Wang, W. F., Guo, J., Guo, H. H., Deng, H. H., Wang, G. B. (2021): Predicting suitable habitats of *Ginkgo biloba* L. fruit forests in China. – Clim Risk Manag 34: 100364.

[16] Fick, S. E., Hijmans, R. J. (2017): WorldClim 2: new 1km spatial resolution climate surfaces for global land areas. – Int J Climatol 37: 4302-4315.

[17] Flowers, T. J., Colmer, T. D. (2008): Salinity tolerance in halophytes. – New Phytol 179: 945-963. https://doi.org/10.1111/j.1469-8137.2008.02531.x.

[18] Garcia-Corral, L. S., Holding, J. M., Carrillo-de-Albornoz, P., Steckbauer, A., Pérez-Lorenzo, M., Navarro, N., Serret, P., Duarte, C. M., Agusti, S. (2017): Effects of UVB radiation on net community production in the upper global ocean. – Glob Ecol Biogeogr 26: 54-64.

[19] Gidden, M. J., Riahi, K., Smith, S. J., Fujimori, S., Luderer, G., Kriegler, E., van Vuuren, D. P., van den Berg, M., Feng, L., Klein, D., Calvin, K., Doelman, J. C. (2019): Global emissions pathways under different socioeconomic scenarios for use in CMIP6: A dataset of harmonized emissions trajectories through the end of the century. – Geosci Model Dev 12: 1443-1475.

[20] Graham, M. H. (2003): Confronting multicollinearity in ecological multiple regression. – Ecology 84: 2809-2815.

[21] IPCC (2013): Climate change 2013: The physical Science Basis. – Contribution of Working Group I to the Fifth Assessment Report of the Intergovernmental Panel on Climate Change. Cambridge University Press, Cambridge, UK and New York, NY, 1535p.

[22] Jamal, Z. A., Abou-Shaara, H. F., Qamar, S., Alotaibi, M. A., Khan, K. A., Khan, M. F., Bashirg, M. A., Hannan, A., AL-Kahtani, S. N., Taha, E. A., Anjum, S. I., Attaullah, M., Raza, G., Ansari, M. J. (2020): Future expansion of small hive beetles, Aethina tumida, towards North Africa and South Europe based on temperature factors using maximum entropy algorithm. – J King Saud Univ Sci 33: 101242.

[23] Jiang, Z., Chen, Y., Ying, B. (2012): Population genetic structure of Tamarix chinensis in the yellow river delta, China. – Plant Syst Evol 298: 147-153.

[24] Jiao, L., Zhang, Y., Sun, T., Yang, W., Shao, D., Zhang, P., Liu, Q. (2021): Spatial analysis as a tool for plant population conservation: a case study of Tamarix chinensis in the Yellow River Delta, China. – Sustainability 13: 8291.

http://www.aloki.hu ● ISSN 1589 1623 (Print) ● ISSN1785 0037 (Online)
DOI: http://dx.doi.org/10.15666/aeer/2004_28452863

[25] Kozak, K. H., Graham, C. H., Wiens, J. J. (2008): Integrating GIS-based environmental data into evolutionary biology. – Trends in Ecology & Evolution 23: 141-148. https://doi.org/10.1016/j.tree.2008.02.001.
[26] Liang, Y., Gillett, N. P., Monahan, A. H. (2020): Climate Model Projections of 21st Century Global Warming Constrained Using the Observed Warming Trend. – Geophysical Research Letters 47(12): e2019GL086757.
[27] Litalien, A., Zeeb, B. (2020): Curing the earth: a review of anthropogenic soil salinization and plant-based strategies for sustainable mitigation. – Sci Total Environ 698: 134235. https://doi.org/10.1016/j.scitotenv.2019.134235.
[28] Liu, W. S., You, J. L., Zeng, W. B., Qi, D. H. (2018): Prediction of the geographical distribution of carex moorcroftii under global climate change based on MaxEnt model. – Chin. J. Grassl. 40(5): 43-49.
[29] Lu, Y. P., Liu, H. C., Chen, W., Yao, J., Huang, Y. Q., Zhang, Y., He, X. Y. (2021): Conservation planning of the genus Rhododendron in Northeast China based on current and future suitable habitat distributions. – Biodivers. Conserv. 30: 673-697.
[30] Munns, R., Tester, M. (2008): Mechanisms of salinity tolerance. – Annual Review of Plant Biology 59: 651-681.
[31] Peng, L. P., Cheng, F. Y., Hu, X. G., Mao, J. F., Xu, X. X., Zhong, Y., Li., S. Y., Xian, H. L. (2019): Modelling environmentally suitable areas for the potential introduction and cultivation of the emerging oil crop Paeonia ostii in China. – Sci Rep 1: 3213.
[32] Peterson, A. T. (2007): Ecological niche modelling and understanding the geography of disease transmission. – Veter Ital 43: 393-400.
[33] Peterson, A. T., Soberón, J., Pearson, R. G., Anderson, R. P., Martínez-Meyer, E., Nakamura, M., Araújo, B. (2011): Ecological niches and geographic distributions. – Princeton University Press: Princeton, NJ, USA.
[34] Phillips, S. J., Anderson, R. P., Schapire, R. E. (2006): Maximum entropy modeling of species geogra-phic distributions. – Ecol Model 190: 231-259.
[35] Phillips, S. J., Dudík, M. (2008): Modeling of species distributions with Maxent: new extensions and a comprehensive evaluation. – Ecography 31: 161-175.
[36] Phillips, S. J., Dudík, M., Schapire, R. E. (2020): Maxent software for modeling species niches and distributions. – Version 3.4.1.
[37] Riahi, K., Vuuren, D. P., Kriegler, E., Edmonds, J., O'Neill, B. C., Fujimori, S., Baue, R. N., Calvin, K., Dellink, R., Fricko, O., Lutz, W. (2017): The Shared Socioeconomic Pathways and their energy, land use, and greenhouse gas emissions implications: An overview. – Glob. Environ. Chang. 42: 153-168.
[38] Rogel, J. A., Ariza, F. A., Silla, R. O. (2000): Soil salinity and moisture gradients and plant zonation in Mediterranean salt marshes of Southeast Spain. – Wetlands 20: 357-372.
[39] Rogelj, J., Meinshausen, M., Knutti, R. (2012): Global warming under old and new scenarios using IPCC climate sensitivity range estimates. – Nat. Clim. Change 2: 248-253.
[40] Rumpf, S. B., Hülber, K., Klonner, G., Moser, D., Schütz, M., Wessely, J., Willner, W., Zimmermann, N. E., Dullinger, S. (2018): Range dynamics of mountain plants decrease with elevation. – Proc Natl Acad Sci 115: 1848-1853.
[41] Santos, J., Al-Azzawi, M., Aronson, J., Flowers, T. J. (2016): eHALOPH a database of salt tolerant plants: helping put halophytes to work. – Plant Cell Physiol 57(1): 1-10. https://doi.org/10.1093/pcp/pcv155.
[42] Song, C. Y., Huang, C., Liu, G. H. (2010): Simulating Potential Distribution of Tamarix chinensis in Yellow River Delta by Generalized Additive Models. – Wetland Science 8: 347-353.
[43] Sun, L. K., Liu, W. Q., Chen, T., Liu, G. X. (2016): Review on mechanism of habitat adaptability and resource value of Tamarix species. – Journal of Desert of Research 36: 349-356.

http://www.aloki.hu ● ISSN 1589 1623 (Print) ● ISSN1785 0037 (Online)
DOI: http://dx.doi.org/10.15666/aeer/2004_28452863

[44] Sun, L. K., Liu, G. X., Zhang, B. G., Zhang, G. S. (2019): Effects of environmental factors on population genetic diversity of Tamarix chinensis. – Acta Prataculturae Sinica 28: 178-186.
[45] Sun, L. K., Liu, G., Lu, Y., Zhang, B., Zhang, G. (2020): Molecular data and ecological niche modelling reveal the phylogeographic pattern of the widespread shrub Tamarix chinensis lour. (Tamaricaceae) in China. – Kew Bull 75: 41.
[46] Valle, J. C. D., Buide, M. L., Whittall, J. B., Valladares, F., Narbona, E. (2020): UV radiation increases phenolic compound protection but decreases reproduction in Silene littorea. – PLoS ONE 15: e0231611.
[47] Wang, H. L., Guo, Y. H., Yang, C. J., Chen, Q. L., Yang, T. X., Zhai, Z. X. (2006): Study on Seed Germination Characteristics of Tamarix chinensis. – China Journal of Chinese Materia Medica 31: 1196-1197.
[48] Wang, W. J., He, H. S., Thompson, F. R., Fraser, J. S., Dijak, W. D. (2017): Changes in forest biomass and tree species distribution under climate change in the northeastern United States. – Landsc Ecol 32: 1399-1413.
[49] Wei, A. Y., Zhang, L., Wang, J. N., Wang, W. W., Niyati, N., Guo, Y. L., Wang, X. F. (2020): Chinese caterpillar fungus (Ophiocordyceps sinensis) in China: current distribution, trading, and futures under climate change and overexploitation. – Sci Total Environ 755: 142548.
[50] Xia, J. B., Lang, Y., Zhao, Q. K., Liu, P., Su, L. (2020): Photosynthetic characteristics of Tamarix chinensis under different groundwater depths in freshwater habitats. – Sci Total Environ 761: 143221.
[51] Xu, M. H., Xue, X. (2013): Analysis on the effects of climate warming on growth and phenology of alpine plants. – J Arid Land Resour Environ 27: 137-141.
[52] Xu, X. X., Cheng, F. Y., Peng, L. P., Sun, Y. Q., Hu, X. G., Li, S. Y., Hong, L. X., Jia, K. H., Abbott, R. J., Mao, J. F. (2019): Late Pleistocene speciation of three closely related tree peonies endemic to the Qinling Daba Mountains, a major glacial refugium in Central China. – Ecology and Evolution 9: 7528-7548.
[53] Xu, N., Meng, F. Y., Zhou, G. F., Li, Y. F., Lu, H. (2020): Assessing the suitable cultivation areas for Scutellaria baicalensis in China using the Maxent model and multiple linear regression. – Biochem Syst Ecol 90: 104052.
[54] Ye, Y., Wang, J., Wang, W., Xu, L-A. (2020): ARF family identification in Tamarix chinensis reveals the salt responsive expression of TcARF6 targeted by miR167. – Peer J 8(4): e8829.
[55] Zelinka, M. D., Myers, T. A., McCoy, D. T., Po-Chedley, S., Caldwell, P. M., Ceppi, P., Klein, S. A., Taylor, K. E. (2020): Causes of higher climate sensitivity in CMIP6 models. – Geo physical Research Letters 47: e2019GL085782. https://doi.org/10.1029/2019GL085782.
[56] Zhang, K. L., Yao, L. J., Meng, J. S., Tao, J. (2018): Maxent modeling for predicting the potential geographical distribution of two peony species under climate change. – Sci Total Environ 634: 1326-1334.
[57] Zhang, R. H., Wen, Q., Xu, L. A. (2019): Development and characterization of genomic SSR markers for Tamarix chinensis (Tamaricaceae). – Appl Plant Sci 7: e1219.
[58] Zhang, H., Song, J. Y., Zhao, H. X., Li, M., Han, W. H. (2021): Predicting the distribution of the invasive species Leptocybe invasa: combining MaxEnt and Geodetector models. – Insects 12: 92.
[59] Zhao, L. C., Zhao, C. Z., Wang, X. P., Wen, J. (2018): Interrelations between environmental factors and distribution of Tamarix gansuensis in Qinwangchuan wetland. – Acta Ecologica Sinica 38: 3422-3431.

http://www.aloki.hu ● ISSN 1589 1623 (Print) ● ISSN1785 0037 (Online)
DOI: http://dx.doi.org/10.15666/aeer/2004_28452863

APPENDIX

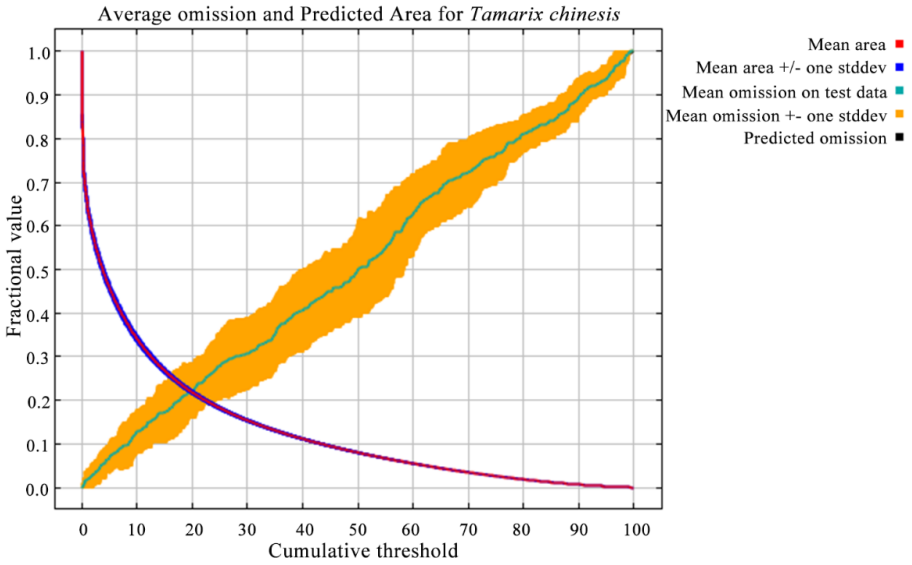

Figure S1. *The omission rate for training and test samples, and predicted area as a function of the cumulative threshold*

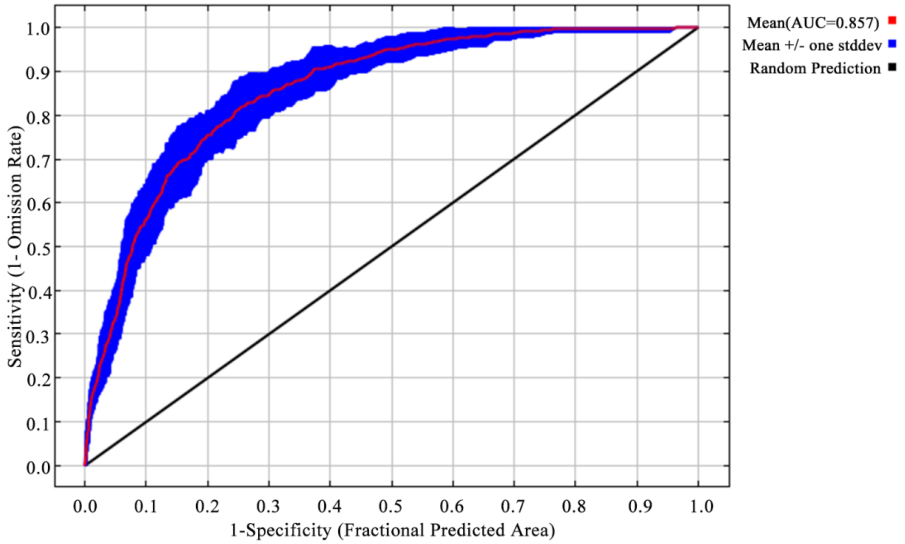

Figure S2. *The curve of receiver operating characteristic for the training and test data*

http://www.aloki.hu ● ISSN 1589 1623 (Print) ● ISSN1785 0037 (Online)
DOI: http://dx.doi.org/10.15666/aeer/2004_28452863

Table S1. *Environmental variables were chosen to model the potential geographic distribution of Tamarix chinensis*

Code	Environmental variables	Unit	Source
Bio1	Annual mean temperature	℃	http://www.worldclim.org/
Bio2	Mean diurnal range	℃	http://www.worldclim.org/
Bio3	Isothermality (BIO2/BIO7) (×100)	×100	http://www.worldclim.org/
Bio4	Temperature seasonality (standard deviation ×100)	×100	http://www.worldclim.org/
Bio5	Max temperature of warmest month	℃	http://www.worldclim.org/
Bio6	Min temperature of coldest month	℃	http://www.worldclim.org/
Bio7	Temperature annual range (BIO5-BIO6)	℃	http://www.worldclim.org/
Bio8	Mean temperature of wettest quarter	℃	http://www.worldclim.org/
Bio9	Mean temperature of driest quarter	℃	http://www.worldclim.org/
Bio10	Mean temperature of warmest quarter	℃	http://www.worldclim.org/
Bio11	Mean temperature of coldest quarter	℃	http://www.worldclim.org/
Bio12	Annual precipitation	mm	http://www.worldclim.org/
Bio13	Precipitation of wettest month	mm	http://www.worldclim.org/
Bio14	Precipitation of driest month	mm	http://www.worldclim.org/
Bio15	Precipitation seasonality (coefficient of variation)	mm	http://www.worldclim.org/
Bio16	Precipitation of wettest quarter	mm	http://www.worldclim.org/
Bio17	Precipitation of driest quarter	mm	http://www.worldclim.org/
Bio18	Precipitation of warmest quarter	mm	http://www.worldclim.org/
Bio19	Precipitation of coldest quarter	mm	http://www.worldclim.org/
Alt	Elevation	m	http://www.gscloud.cn/
Slop	Slope	°	http://www.gscloud.cn/
Asp	Aspect	°	http://www.gscloud.cn/
T_OC	Topsoil organic carbon	% weight	http://globalchange.bnu.edu.cn/research/soil2）
T_PH_H2O	Topsoil pH (H2O)	-log(H+)	http://globalchange.bnu.edu.cn/research/soil2）
T_TEB	Topsoil TEB	cmol/kg	http://globalchange.bnu.edu.cn/research/soil2）
T_USDA_TEX_CLASS	Topsoil USDA texture classification	name	http://globalchange.bnu.edu.cn/research/soil2）
UVB1	Annual mean UV-B	J m-2 •day-1	http://www.ufz.de/gluv/
UVB2	UV-B seasonality	J m-2 •day-1	http://www.ufz.de/gluv/
UVB3	Mean UV-B of lightest month	J m-2 •day-1	http://www.ufz.de/gluv/
UVB4	Mean UV-B of lowest month	J m-2 •day-1	http://www.ufz.de/gluv/

http://www.aloki.hu ● ISSN 1589 1623 (Print) ● ISSN1785 0037 (Online)
DOI: http://dx.doi.org/10.15666/aeer/2004_28452863

Table S2. *Correlation matrix between fourteen variables used in ENM test*

Variables	BIO1	BIO7	BIO14	BIO15	BIO16	T_OC	PH	TED	USDA	UVB1	UVB2	ALT	aspect	slope
BIO1	1													
BIO7	-0.436	1												
BIO14	0.625	-0.575	1											
BIO15	-0.533	0.3719	-0.601	1										
BIO16	0.586	-0.6599	0.749	-0.267	1									
T_OC	-0.131	-0.1359	0.070	0.015	0.12312	1								
PH	0.005	0.3579	-0.301	0.128	-0.30525	-0.20534	1							
TED	0.033	0.289	-0.199	0.065	-0.24648	0.01339	0.70543	1						
USDA	-0.368	0.2813	-0.442	0.260	-0.44138	-0.19742	0.02345	-0.20844	1					
UVB1	-0.304	-0.5243	-0.060	0.025	-0.06985	0.16508	-0.33669	-0.26159	0.14413	1				
UVB2	-0.684	0.033	-0.469	0.258	-0.57147	0.10392	-0.10055	-0.07518	0.36433	0.77752	1			
ALT	-0.354	-0.098	-0.185	0.132	-0.18525	0.0849	-0.12141	-0.10272	0.15216	0.44031	0.46335	1		
aspect	-0.005	0.001	0.014	-0.017	0.01001	0.00802	-0.0061	0.00805	-0.00922	0.00507	-0.00247	0.00348	1	
slope	-0.03967	-0.02251	-0.01261	-0.00861	-0.00473	0.00144	-0.05172	-0.04079	0.01934	0.0515	0.04312	0.03414	0.09452	1

http://www.aloki.hu ● ISSN 1589 1623 (Print) ● ISSN1785 0037 (Online)
DOI: http://dx.doi.org/10.15666/aeer/2004_28452863